Wave-inspired Corrections for an Efficient Ray-optical Description of Micro-optics Devices

P. Stockschläder, J. Kreismann, and M. Hentschel
Institute for Physics, Technische Universität Ilmenau, Ilmenau, Germany

Abstract— Ray optics is a versatile tool to describe microscale optical systems like microlasers and their far-field emission. It is successful even in the regime where a wave-dynamical description would be expected to be appropriate. Indeed, when considering structures at length scales of a few light wavelengths, wave-inspired adjustments have to be taken into account to ensure the accuracy of ray-based predictions. These corrections to ray optics are known as the Goos-Hänchen shift, a lateral shift along the interface, and the Fresnel filtering effect, an angular shift, violating Snells law and the principle of ray-path reversibility. In this contribution, we study in detail the influences of different factors on the exact size of the corrections paying special attention to the interplay between beam parameters and interface geometry. We obtain our results from analytical calculations using an expectation value approach to the beam shifts. These findings are supported by FDTD simulations. Knowing the influences of the different parameters, we are able to incorporate well adjusted correction terms in the ray-optical calculations for a large class of micro-optics devices with curved and planar boundaries.

1. INTRODUCTION

Optical microlasers and microcavities have attracted much interest because of their application potential in photonic and optoelectronic devices [1–3]. For the description of these micro-optics devices the concept of ray-wave correspondence has proven useful [4–6]. This concept uses geometrical optics to predict the modes and the far-field emission pattern of the devices [5, 7]. However, deviations from ray-optics occur as the system size becomes of the order of the light wavelength [8]. These deviations have to be taken into account to obtain accurate results [9].

The corrections to the laws of reflection and refraction are known as Goos-Hänchen shift [10–12] and Fresnel filtering [13]. The two contributions act in different directions in phase space [14]: The Goos-Hänchen shift (GHS) denotes a lateral shift of the reflected light beam along the interface. The Fresnel filtering (FF) effect describes a correction of Snell's law and acts on the angle of the reflected light, i.e., its momentum.

For an intuitive understanding of these effects at planar interfaces refer to Fig. 1(a) [15]. The Goos-Hänchen shift at a planar interface occurs primarily for total internal reflection (incident angle $\chi_{\rm in}$ larger than the critical angle $\chi_c = \arcsin(1/n)$ whith the relative refractive index $n = n_1/n_2$). It results from an interference effect [11] and yields a lateral shift along the interface of the order of the vacuum light wavelength λ between incident and reflected beam [12, 16, 17]. Due to the finite penetration depth γ, of the order of λ, of totally reflected light into the optically thinner medium,

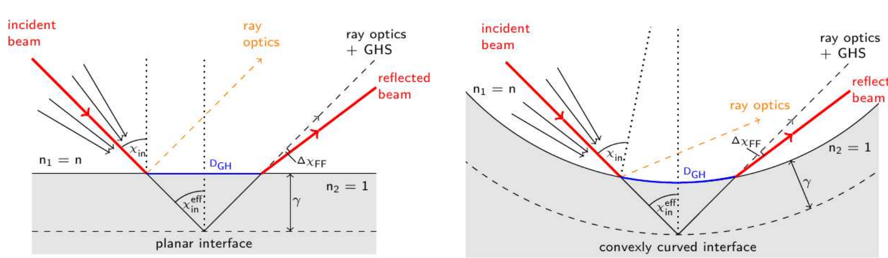

(a) (b)

Figure 1: Schematic picture of the beam shifts at (a) planar, (b) curved interfaces. Incident and reflected beam are shown in red. The relative refractive index is $n = n_1/n_2$. The effective interface is depicted as dashed line, γ is the penetration depth. The normals to the interface and the effective interface (dotted lines) define the angle of incidence $\chi_{\rm in}$ and the effective angle of incidence $\chi_{\rm in}^{\rm eff}$. The reflected beam predicted from ray optics is shown as dashed orange arrow. The lateral shift along the interface $D_{\rm GH}$ due to the Goos-Hänchen effect (blue) and the angular deflection $\Delta\chi_{\rm FF}$ due to the Fresnel filtering effect are marked.

the reflection can be assumed to occur at an effective interface (dashed line in Fig. 1) under an effective angle of incidence $\chi_{\rm in}^{\rm eff}$ [18, 19]. The lateral shift is estimated to $D_{\rm GH} = 2\gamma\tan(\chi_{\rm in}^{\rm eff})$.

The Fresnel filtering [13] (or angular Goos-Hänchen shift, [14, 20–23]) has its origin in the finite spatial extent of a light *beam* as opposed to the light *rays* of geometrical optics. This finite beam width induces angles of incidence distributed around a mean $\chi_{\rm in}$. Now, suppose $\chi_{\rm in} = \chi_c$. All smaller angles in the distribution will be partially transmitted, whereas all larger angles will be totally reflected – the mean angle of the reflected light will deviate from $\chi_{\rm in}$: Snell's law is violated, $\chi_{\rm out} = \chi_{\rm in} + \Delta\chi_{\rm FF}$, with the FF correction $\Delta\chi_{\rm FF}$. Consequently, FF will be most important around χ_c and for beams narrow in space, i.e., with a broad angular distribution.

At a curved interface, schematically depicted in Fig. 1(b), the beam shifts can be qualitatively understood in the same manner, though, with two major differences. Whereas $\chi_{\rm in}^{\rm eff} = \chi_{\rm in}$ holds at a planar interface, we find $\chi_{\rm in}^{\rm eff} < \chi_{\rm in}$ in the convexly curved case. As we can still approximate the GHS to be $D_{\rm GH} \approx 2\gamma\tan(\chi_{\rm in}^{\rm eff})$, we expect the lateral shift to be smaller with increasing curvature. Furthermore, the angular spread of the incident light beam is effectively enhanced by the interface curvature which will lead to an increased FF at curved interfaces.

2. METHODOLOGY

Here, we use an expectation value approach to the beam shifts [15, 24] which is more widely applicable than the different approximative formulas discussed in literature [11, 12, 16, 22].

In the planar case, the beam is expanded in plane waves. We restrict our calculations to the interface, denoted by the z-axis. The incident beam is given by $E_I(z) = \int {\rm d}k_z e_I(k_z){\rm e}^{{\rm i}k_z z}$, where the transverse beam profile $e_I(k_z)$ is supposed to be centered about one momentum component $k_z = k_0$ corresponding to the central angle of incidence $\chi_{\rm in}$ via $k_z = k\sin(\chi)$ with the wavenumber $k = 2\pi/\lambda$. The reflected beam is obtained by applying the Fresnel reflection coefficients [25] to the incident beam profile, $e_R(k_z) = \rho(k_z)e_I(k_z)$ leading to $E_R(z) = \int {\rm d}k_z e_R(k_z){\rm e}^{{\rm i}k_z z}$.

The beam shifts can then be defined as expectation values of the reflected beam:

$$D_{\rm GH} = \langle z\rangle = \frac{\int_{-\infty}^{\infty}{\rm d}z E_R^*(z) z E_R(z)}{\int_{-\infty}^{\infty}{\rm d}z\,|E_R(z)|^2} \quad \text{and} \quad \Delta k_{\rm FF} = \langle k_z - k_0\rangle = \frac{\int {\rm d}k_z e_R^*(k_z)(k_z-k_0)e_R(k_z)}{\int {\rm d}k_z\,|e_R(k_z)|^2}. \quad (1)$$

From the shift in momentum $\Delta k_{\rm FF}$, the angular deflection is obtained as $\Delta\chi_{\rm FF} = \arcsin(\Delta k_{\rm FF}/k)$.

For curved interfaces, we concentrate on circularly symmetric systems. Any curved boundary can be locally approximated by a circle. The beams are conveniently expanded in polar coordinates (r, α) using Bessel functions. Angular momentum conservation leads to a relation between the angular wavenumber m of the cylinder function J_m and the angle of incidence χ, $\sin(\chi) = m/(nkR)$ [18]. The incident light beam at the interface $r = R$, then, is $E_I(\alpha) = \sum_m e_I(m){\rm e}^{{\rm i}m\alpha}J_m(nkR)$. The transverse beam profile in angular momentum space $e_I(m)$ is chosen to be strongly peaked at the central angular wavenumber m_0 corresponding to $\chi_{\rm in}$. The reflected beam is obtained by applying the corrected Fresnel reflection coefficients for convexly curved interfaces [25] to the incident beam profile, $e_R(m) = \rho_c(m)e_I(m)$, giving $E_R(\alpha) = \sum_m e_R(m){\rm e}^{{\rm i}m\alpha}J_m(nkR)$.

Here, the beam shifts are obtained from the expectation values of the polar angle and the angular wavenumber

$$\Delta\alpha_{\rm GH} = \langle\alpha\rangle = \frac{\int_{-\pi}^{\pi}{\rm d}\alpha E_R^*(\alpha)\alpha E_R(\alpha)}{\int_{-\pi}^{\pi}{\rm d}\alpha E_R^*(\alpha)E_R(\alpha)} \text{ and } \Delta m_{\rm FF} = \langle m - m_0\rangle = \frac{\sum_m e_R^*(m)(m-m_0)e_R(m)}{\sum_m e_R^*(m)e_R(m)}. \quad (2)$$

The lateral shift $D_{\rm GH}$ along the interface, given in multiples of the vacuum wavelength λ, is then $D_{\rm GH} = nkR\,\Delta\alpha_{\rm GH}/(2\pi)$ and the angular deflection is $\Delta\chi_{\rm FF} = \arcsin(\Delta m_{\rm FF}/(nkR))$.

As transverse beam profiles we choose a Gaussian in momentum and angular momentum space for the planar and curved case, respectively,

$$e_I(k_z) = \frac{1}{\sqrt{2\pi}\epsilon}{\rm e}^{-\frac{(k_z-k_0)^2}{2\epsilon^2}} \quad \text{and} \quad e_I(m) = \frac{1}{\sqrt{2\pi}\sigma}{\rm e}^{-\frac{(m-m_0)^2}{2\sigma^2}} \quad (3)$$

with corresponding beam waists in real space $w/\lambda = \sqrt{2}k/(\pi\epsilon)$ and $w/\lambda = \sqrt{2}kR/(\pi\sigma)$.

Numerical results are obtained from full electromagnetic calculations simulating a Gaussian beam incident on planar and curved dielectric interfaces, see Fig. 2. These simulations have been

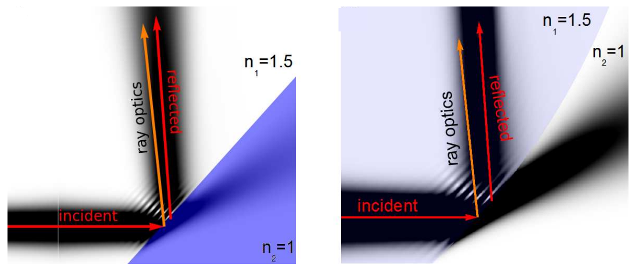

(a) (b)

Figure 2: Real space pictures of a Gaussian beam with width $w/\lambda = 5$ reflected at a dielectric interface with relative refractive index $n = 1.5$ near critical incidence. The direction of incident and reflected beams are given by red arrows, the direction of the reflected beam expected from ray optics is given by the orange arrow. (a) TM polarized beam at a planar interface. (b) TE polarized beam at a curved interface with $kR = 400$.

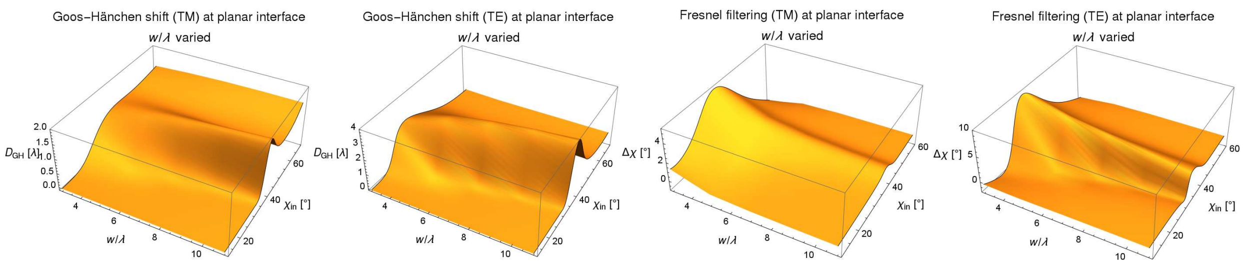

Figure 3: Effect of the beam waist on the beam shifts at a planar interface. The wavenumber k is fixed while the beam waist w/λ is varied. Goos-Hänchen shift and the Fresnel-filtering effect according to Equation (1) are shown for both, TM and TE, polarization. The relative refractive index is $n = 1.5$, $\chi_c \approx 41.8$, $\chi_B \approx 33.7$.

performed with the finite-difference time-domain (FDTD) method, using a freely available software package [26]. The ray propagation directions of the incident and reflected beams are obtained as mean value of the Poynting vectors and are denoted by red arrows. The deviation from geometrical optics, marked by the orange arrow, is clearly visible. The beam shifts are calculated as the difference between the simulated reflected beam and its ray-optics expectation.

3. RESULTS AND DISCUSSION

Now, we discuss the influence of the different parameters on the beam shifts. One important parameter is the beam width. At curved interfaces, the radius of curvature, additionally, is crucial.

In Fig. 3, the dependence on beam width of GHS and FF at planar interfaces is depicted. Firstly, both effects are broadened with reduced beam width, thus, giving a contribution for a larger range of incident angles. Secondly, GHS increases while FF decreases with increasing beam width. This is understood in the intuitve picture described in the Introduction. GHS depends on the spatial extent of the beam, whereas, FF depends on the width of the angular distribution. A broader beam in space corresponds to a narrower angular spectrum. The effects are strongest around the critical angle and the GHS has a finite value for supercritical incidence, whereas, FF drops to zero in this regime. We expect the least deviations from ray-optics for subcritical incidence, and this is indeed seen for TM polarization. The TE result, however, has a distinct contribution there, which is due to the Brewster angle, $\chi_B = \arctan(1/n) < \chi_c$, where no TE polarized light is reflected.

In Fig. 4, the effect of curvature on GHS and FF at convexly curved interfaces is studied. The radius of curvature R is changed while the angular spread σ and the beam width w/λ are kept fixed in Fig. 4(a) and 4(b), respectively. The results confirm the predictions made in the intuitive picture. When the radius is decreased, the effective angle of incidence is lower, thus, the GHS decreases in both cases. For the FF, however, the situation is more involved. In the case of fixed angular spread in the beam (Fig. 4(a)), the effective angular spread with respect to the interface is increased at a more strongly curved interface. Hence, the FF increases with decreasing radius. In the case of fixed beam width (Fig. 4(b)), however, σ changes, according to $w/\lambda = \sqrt{2kR}/(\pi\sigma)$, linearly with the radius of curvature when k and w/λ are fixed. Hence, the angular spread is increased by the same amount as the curvature is reduced. Consequently, the FF is unchanged in absolute size, only the position of the maximum is shifted and the features are broader for smaller R.

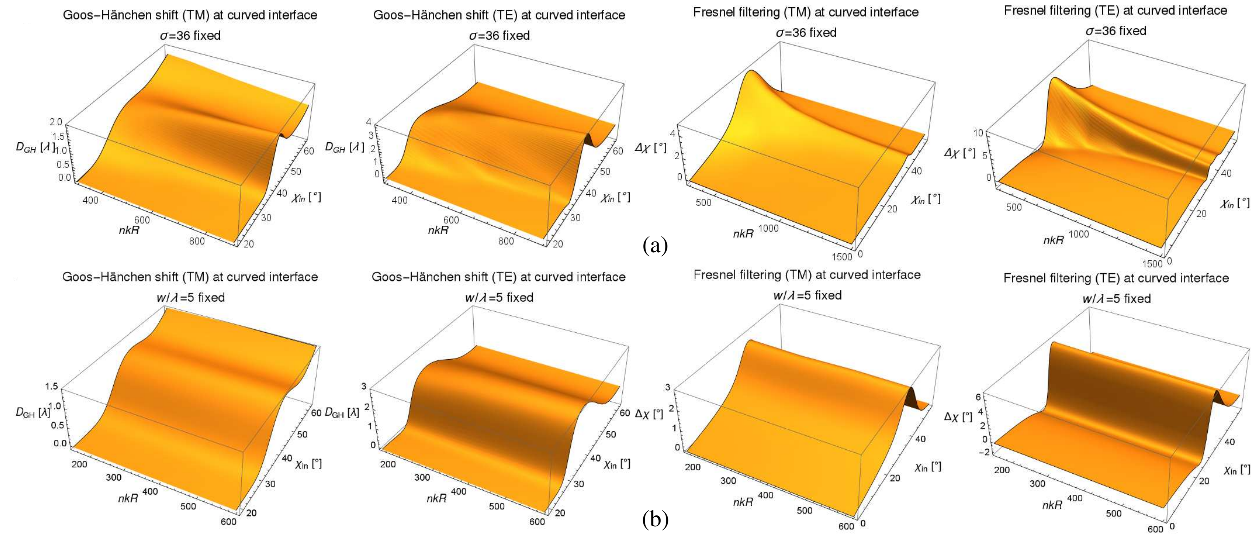

Figure 4: Effect of (a) angular spread and (b) beam waist on the beam shifts at convex interfaces. The wavenumber k and (a) the angular spread $\sigma = 36$, (b) the beam waist $w/\lambda = 5$ are fixed while the curvature $\kappa = 1/R$ is varied. Goos-Hänchen shift and the Fresnel-filtering effect according to Equation (2) are shown for both, TM and TE, polarization. The relative refractive index is $n = 1.5$, $\chi_c \approx 41.8$, $\chi_B \approx 33.7$.

4. CONCLUSION

For the inclusion of the correction terms in a ray-optical description of micro-optics devices, it is important to know how GHS and FF affect the prediction of the far-field emission. In polygonal microcavities which have only planar boundaries, only FF plays a role as it affects the emission direction. Whereas, GHS leads only to a parallel shift of the rays but not to a change in direction. For all other geometries with curved and mixed boundaries, both effects are important. Although GHS is diminished at strongly curved interfaces it still has to be taken into account as the shift along a curved boundary also affects the direction of the resulting beam. However, FF is of special importance here as it is strongly increased with curvature. Hence, it has a large impact on the prediction of the emission direction.

Furthermore, both effects are broadened with increasing curvature, thus, being important in a larger range of incident angles also far away from the critical angle. Especially in experiments with TE polarized light, the enhancement of the beam shift corrections and their Brewster angle features might lead to far-field patterns that deviate from the ray-optics expectation (e.g., [27, 28]).

Knowing the influence of polarization, beam width, angular spread and boundary curvature on the beam shift effects GHS and FF, we are now able to incorporate them in the ray-optical calculations for a large class of micro-optics devices with curved and planar boundaries. Thus, we can make predictions for these devices exploiting the simplicity and efficiency of geometrical optics while keeping the accuracy of wave calculations.

ACKNOWLEDGMENT

The authors gratefully acknowledge funding by the German Research Society (DFG) via the Emmy Noether Program and the Research Unit FOR 760. We thank Daniel Kotik, Jörg Götte, Ulf Peschel, and Henning Schomerus for discussions and valuable advice.

REFERENCES

1. Chang, R. K., *Optical Processes in Microcavities*, World Scientific, Singapore, 1996.
2. Vahala, K., *Optical Microcavities*, World Scientific, Singapore, 2004.
3. Cao, H. and J. Wiersig, "Dielectric microcavities: Model systems for wave chaos and non-Hermitian physics," *Rev. Mod. Phys.*, Vol. 87, No. 1, 61–111, 2015.
4. Schwefel, H. G. L., N. B. Rex, H. E. Tureci, R. K. Chang, A. D. Stone, T. Ben-Messaoud, and J. Zyss, "Dramatic shape sensitivity of directional emission patterns from similarly deformed cylindrical polymer lasers," *J. Opt. Soc. Am. B*, Vol. 21, No. 5, 923–934, 2004.
5. Wiersig, J. and M. Hentschel, "Combining directional light output and ultralow loss in deformed microdisks," *Phys. Rev. Lett.*, Vol. 100, No. 3, 033901, 2008.

6. Hentschel, M. and K. Richter, "Quantum chaos in optical systems: The annular billiard," *Phys. Rev. E*, Vol. 66, No. 5, 056207, 2002.
7. Tanaka, T., M. Hentschel, T. Fukushima, and T. Harayama, "Classical phase space revealed by coherent light," *Phys. Rev. Lett.*, Vol. 98, No. 3, 033902, 2007.
8. Song, Q. H., L. Ge, A. D. Stone, H. Cao, J. Wiersig, J.-B. Shim, J. Unterhinninghofen, W. Fang and G. S. Solomon, "Directional laser emission from a wavelength-scale chaotic microcavity," *Phys. Rev. Lett.*, Vol. 105, No. 10, 103902, 2010.
9. Altmann, E. G., G. Del Magno, and M. Hentschel, "Non-Hamiltonian dynamics in optical microcavities resulting from wave-inspired corrections to geometric optics," *EPL*, Vol. 84, No. 1, 10008, 2008.
10. Goos, F. and H. Hänchen, "Ein neuer und Fundamentaler Versuch Zur Totalreflexion," *Annalen der Physik*, Vol. 436, No. 7-8, 333–346, 1947.
11. Artmann, K., "Berechnung der Seitenversetzung des totalreflektierten Strahles," *Annalen der Physik*, Vol. 437, No. 1-2, 87–102, 1948.
12. Lai, H. M., F. C. Cheng, and W. K. Tang, "Goos-Hänchen effect around and off the critical angle," *J. Opt. Soc. Am. A*, Vol. 3, No. 4, 550–557, 1986.
13. Tureci, H. E. and A. D. Stone, "Deviation from Snell's law for beams transmitted near the critical angle: Application to microcavity lasers," *Opt. Lett.*, Vol. 27, No. 1, 7–9, 2002.
14. Schomerus, H. and M. Hentschel, "Correcting ray optics at curved dielectric microresonator interfaces: Phase-space unification of Fresnel filtering and the Goos-Hänchen shift," *Phys. Rev. Lett.*, Vol. 96, No. 24, 243903, 2006.
15. Stockschläder, P., J. Kreismann, and M. Hentschel, "Curvature dependence of semiclassical corrections to ray optics: How Goos-Hänchen shift and Fresnel filtering deviate from the planar case result," *EPL*, Vol. 107, No. 6, 64001, 2014.
16. Horowitz, B. R. and T. Tamir, "Lateral displacement of a light beam at a dielectric interface," *J. Opt. Soc. Am.*, Vol. 61, No. 5, 586–594, 1971.
17. Lotsch, H. K. V., "Beam displacement at total reflection: The Goos-Hänchen effect I," *OPTIK*, Vol. 32, No. 2, 116–137, 1970.
18. Hentschel, M. and H. Schomerus, "Fresnel laws at curved dielectric interfaces of microresonators," *Phys. Rev. E*, Vol. 65, No. 4, 045603, 2002.
19. Kotik, D. and M. Hentschel, "How curvature affects the far-field emission from deformed optical microcavities," *J. Opt.*, Vol. 15, No. 1, 014010, 2013.
20. Merano, M., A. Aiello, M. P. van Exter, and J. P. Woerdmann, "Observing angular deviations in the specular reflection of a light beam," *Nat. Photon.*, Vol. 3, No. 6, 337–340, 2009.
21. Fiedler-Ferrari, N., H. M. Nussenzveig, and W. J. Wiscombe, "Theory of near-critical-angle scattering from a curved interface," *Phys. Rev. A*, Vol. 43, No. 2, 1005–1038, 1991.
22. Bliokh, K. Y. and A. Aiello, "Goos-Hänchen and Imbert-Fedorov beam shifts: An overview," *J. Opt.*, Vol. 15, No. 1, 014001, 2013.
23. Götte, J. B., S. Shinohara, and M. Hentschel, "Are Fresnel filtering and the angular Goos-Hänchen shift the same?," *J. Opt.*, Vol. 15, No. 1, 014009, 2013.
24. Porras, M. A., "Moment-method evaluation of the angular and lateral shifts of reflected light beams," *Opt. Commun.*, Vol. 131, No. 1-3, 13–20, 1996.
25. Jackson, J. D., *Classical electrodynamics*, 3 Edition, Wiley, New York, 1999.
26. Oskooi, A. F., D. Roundy, M. Ibanescu, P. Bermel, J. D. Joannopoulos, and S. G. Johnson, "MEEP: A flexible free-software package for electromagnetic simulations by the FDTD method," *Comput. Phys. Commun.*, Vol. 181, No. 3, 687–702, 2010.
27. Song, Q., W. Fang, B. Liu, S.-T. Ho, G. S. Solomon, and H. Cao, "Chaotic microcavity laser with high quality factor and unidirectional output," *Phys. Rev. A*, Vol. 80, No. 4, 041807, 2009.
28. Shinohara, S., M. Hentschel, J. Wiersig, T. Sasaki, and T. Harayama, "Ray-wave correspondence in limaçon-shaped semiconductor microcavities," *Phys. Rev. A*, Vol. 80, No. 3, 031801, 2009.